Mediodorsal thalamus contributes to the timing of instrumental actions

Authors/Affiliations:

Nicholas Lusk[1], Warren H. Meck[1], Henry H. Yin[1,2,†]

1. Department of Psychology and Neuroscience; Duke University; Durham, NC, 27708; USA.,
2. Department of Neurobiology; Duke University School of Medicine; Durham, NC, 27708; USA.

†**Correspondence**: hy43@duke.edu

Abstract:

The ability to represent time in the brain relies on network interactions across multiple brain areas. While much attention has been paid to the role of prefrontal cortex and basal ganglia in timing, little work has been aimed towards understanding the role of the thalamus in timing. To this end, we utilized pharmacological and optogenetic techniques in mice to test the role of the mediodorsal nucleus of the thalamus (MD) in interval timing. The MD is strongly connected with the prefrontal cortex and receives major inputs from the basal ganglia output nuclei. We used an operant temporal production task, in which mice indicate their expected timing of available rewards by pressing a lever in anticipation. On probe trials, inactivation of the MD with muscimol produced rightward shifts in peak pressing as well as increases in peak spread, thus significantly altering both temporal accuracy and precision. Optogenetic inhibition of glutamatergic projection neurons in the MD resulted in similar changes in timing; the shift in peak time is proportional to the duration of inhibition. The observed effects were found to be independent of significant changes in movement. Taken together, these findings provide strong evidence for the importance of thalamo-cortical projections in maintaining proper timing behavior.

Significance Statement: While extensive research has been dedicated to the involvement of the prefrontal cortex in interval timing behavior, the degree to which thalamic inputs contribute to timing is unclear. Using pharmacological and optogenetic inhibition of the MD, a prefrontal projecting thalamic nucleus, we demonstrate a key role of this thalamic nucleus in timing behavior.

Introduction:

The ability to track the passage of time is ubiquitous across the animal kingdom and vital for survival (Buhusi and Meck, 2005). Neural correlates of timing have been found across the cortex as well as the basal ganglia (Meck, 2006; Kim et al., 2013; Yin, 2014; Finnerty et al., 2015; Gouvea et al., 2015; Bakhurin et al., 2017; Tiganj et al., 2017). However, how these regions work together to produce a unified perception of time remains unclear (Lewis and Miall, 2003; Teki et al., 2012).

A critical component of cortico-basal ganglia circuits is the thalamus, but the role of the thalamus in timing remains poorly understood. Recent work has focused on the role of the prefrontal cortex (PFC) in timing (Jones et al., 2004; Buhusi et al., 2018; Kim and Narayanan, 2019). In rodents, the PFC is defined largely by the existence of strong reciprocal connections with the mediodorsal nucleus (MD) of the thalamus (Heidbreder and Groenewegen, 2003). The MD not only receives strong projections from the basal ganglia, but also send massive glutamatergic projections that drive feed-forward inhibition within the PFC (Delevich et al., 2015). It is thus in a position to serve as a key node in the interval timing circuit. The MD has also been implicated in acquisition and selection of instrumental actions controlled by action-outcome contingencies (Corbit et al., 2003; Ostlund and Balleine, 2008; Yu et al., 2012; Parnaudeau et al., 2013; Parnaudeau et al., 2015). Recent optogenetic work has demonstrated interactions between PFC and MD to be crucial for performance on working memory tasks in rodents (Bolkan et al., 2017; Ferguson and Gao, 2018). Moreover, work in non-human primates as well as rodents has found deficits in acquisition and execution of sub-second timing after disruption of PFC projecting thalamic neurons (Yu et al., 2010; Wang et al., 2018). The MD-PFC circuit has been implicated in the maintenance of working memory.

In this study, we use pharmacological and optogenetic techniques in mice to examine the role of the MD in time perception. We selectively inhibited the MD during a temporal production task, using local infusions of muscimol, a GABA-A receptor agonist. MD inhibition reduced temporal precision. Optogenetic inhibition of glutamatergic projection neurons in the MD demonstrated state-dependent effects, with animals perseverating in their behavior at time of stimulation. This resulted in rightward shifts in peak pressing when stimulation was present at the onset of trials, and lengthened pressing when stimulation was paired with lever pressing. These effects were independent of changes in general motor activity.

Results:

Pharmacological inhibition of MD

Mice (n = 10, C57BL/6) were implanted with guild cannulas prior to being trained on a 30s peak interval procedure (Figure 1A). Following experimentation, localization of cannula placement was verified for all animals (Figure 1B). After progressing to the final stage of training (see Materials & Methods) animals were assigned an infusion schedule, counterbalanced across subjects. Session averaged response rates during non-rewarded probe trials were normalized in amplitude and fit using a Gaussian + Ramp function. Control animals exhibited peak times at (26.33s ± 1.32s) for the 30s PI procedure, which was significantly lower than the 30s criteria, but in alignment with previous work in mice on the same task (Buhusi et al., 2009). The peak functions revealed differences between muscimol and control conditions (Figure 1C). Repeated measures one-way ANOVA found significant effect of treatment on peak time ($F(1.953, 17.58) = 10.65$, $p < 0.001$) and variance ($F(1.878, 16.90) = 20.25$, $p < 0.001$). A Tukey's post hoc test revealed significant increases in the muscimol peak time (33.46s ± 1.183s) and variance (15.86s ± 0.915s) relative to control (26.33s ± 1.32s, $p = 0.002$; 10.37s ± 0.342s, $p < 0.001$) as well as saline (29.19s ± 1.39s, $p = 0.05$; 12.07s ± 0.592s, $p = 0.01$). No significant differences were found between control and saline conditions for either peak time ($p = 0.251$) or variance ($p = 0.139$).

To shed light on behavioral patterns that give rise to the session averaged data shown in Figure 1, we conducted a single trial analysis. For each trial, the start time, stop time, and duration of lever pressing was calculated (Figure 2A). This analysis revealed significant increases in the stop time ($t(81) = 6.217$; $p < 0.001$; $t(81) = 4.053$, $p < 0.001$) as well as duration of pressing ($t(81) = 5.431$, $p < 0.001$; $t(81) = 4.44$, $p < 0.001$) for the muscimol condition compared to control and saline conditions, respectively (Figure 2B). The distribution of inter-press-intervals (IPIs), a metric of pressing structure, shows qualitatively similar profiles between muscimol (0.69 ± 0.0044 s, SD = 0.398s) and saline (0.65 ± 0.0033, SD = 0.332s) conditions (Figure 2C).

No significant difference in total lever presses was found between groups ($F(2, 18) = 0.77$, $p = 0.478$), indicating increases in response variance could not be solely explained by differences in the level of motor output by muscimol animals (Figure 2D). However, animals had significantly lower elevation ratios (i.e. trial presses / total presses) based on treatment ($F(1.458, 13.12) = 21.93$, $p < 0.001$), with the muscimol condition (0.703 ± 0.035) being significantly lower than both control (0.8691 ± 0.022, $p < 0.001$) and saline (0.8319 ± 0.015, $p = 0.007$) conditions (Figure 2D). Therefore, while the muscimol doses given in this study did not significantly change overall lever pressing, it did alter the animal's ability to distinguish between which states during the task would produce rewarded press.

Optical inhibition of MD

While pharmacological inhibition of the MD demonstrated its importance to proper timing behavior, how the MD activity contributes to individual behavioral phases during a PI procedure remains unanswered. A given trial can be divided into three phases: initial "low-state" followed a pressing "high-state" and concluding with a second "low-state" (Church et al., 1994). To investigate the contributions of MD to behavior with higher temporal resolution, we used optogenetics to inactivate the MD (Figure 3A-B). We used a Cre-dependent halorhodopsin (DIO-eNpHR3.0) in vGlut2-Cre mice to selectively inhibit vGlut2+ projection neurons in the MD (Zhang et al., 2007). This manipulation provides more spatially and temporally selective inactivation of the MD. Spatially, it is limited to the glutamatergic projection neurons; temporally it can be used at specific time points during the trial. We selected three timepoints for inhibition (0s, 15s, and 60s). Each timepoint occurs primarily during one of the three phases. Inhibition was constant over 15s as this has previously been shown to effectively disrupt prefrontal dependent processes such as working memory maintenance (Bolkan et al., 2017).

Performance on non-laser trials was consistent with previous work. Peak time (25.53s ± 0.719s) was significantly lower than 30s, but not significantly different than control data from muscimol experiments ($t(14) = 0.4416$, $p = 0.6655$), nor was the peak variance ($t(14) = 0.841$, $p = 0.4145$). Therefore, despite having MD inhibition on 50% of the reward trials, there is likely no residual influence on non-laser peak trials. When optical inhibition was concurrent with the onset of the trial, animals produced a systematic delay in the onset of lever pressing, evidenced by a

rightward shift in peak time (Figure 3C). However, the rightward shift in peak times ($t(5) = 9.051$, $p < 0.001$) was not accompanied by a significant difference in temporal variance ($t(5) = 1.312$, $p = 0.2465$: Figure 3D). Single trial analysis demonstrated the rightward shift to be a product of delays in the start ($t(15) = 4.198$, $p = 0.002$) and stop ($t(15) = 3.594$, $p = 0.008$) of the pressing high-state with no changes in the duration of pressing ($t(15) = 0.6045$, $p = 0.912$: Figure 3E). A 2-dimensional density plot shows qualitative similarities in the distribution of start and stop times (Figure 3F). Despite having significantly different means, an F-test for equality of variance found no significant differences between the two conditions for start times ($F(140, 124) = 1.06$, $p = 0.5669$) or stop times ($F(124, 140) = 1.303$, $p = 0.1284$).

To assess how MD inhibition modulates behavior during the pressing high-state, inhibition was started 15s into the trial. Average start times during non-laser trials for the t = 0s condition (11.232s ± 1.001s) indicated this to be a likely time for mice to be in the early stages of their pressing high-state. As with optical inhibition at onset, animals produce rightward shifts in peak pressing ($t(5) = 5.35$, $p = 0.0031$), but this was accompanied by a significant increase in peak variance ($t(5) = 4.788$, $p = 0.0049$: Figure 4A-B). Single trial analysis was again done in order to evaluate the contributing factors to differences found in session averaged data between conditions (Figure 4C). Contrary to the effects seen with inhibition at trial onset, inhibition at t = 15s produced significant delays in pressing stop times ($t(15) = 4.191$, $p = 0.002$) as well as increases in the duration of the pressing high-state ($t(15) = 3.942$, $p = 0.004$) with no significant differences in start times ($t(15) = 0.2408$, $p = 0.993$). In addition to the increases in mean length of pressing, how inhibition of the MD affected the variability of press duration was investigated through assessment of Gaussian fits of press duration histograms (Figure 4D). An extra sum-of-squares F-test found the variance of the inhibition condition's best fits to be significantly greater than that of non-inhibition trials ($F(1, 32) = 15.14$, $p = 0.0005$). Therefore, inhibition of the MD does not only lead to increased duration of pressing, but also increased variability in the length of a pressing bout.

As the start of the lever pressing bout (high state) can vary from trial to trial, A linear regression was performed between the bout duration and total amount of inhibition as a fraction of the possible 15s (Figure 4E). When only part of the inhibition occurred during pressing, no distinction was made between whether inhibition occurred at the beginning or end of the pressing. The fraction of inhibition showed a strong linear correlation with duration of the lever

pressing bout ($R2 = 0.6136$) and demonstrated a significantly positive slope ($F(1, 13) = 20.64$, $p < 0.001$).

The final time point for optical inhibition, t = 60s, occurs after the animal has finished pressing. As expected, inhibition at this point has no significant effects on performance (session averaged, Figures 5A-B; single trial, Figures 5C). However, mice exhibited a significant increase in rebound pressing during inhibition trials (Figure 5D: $t(4) = 3.296$, $p = 0.0301$). This is unlikely to be explained by confounding factors such as visually perceiving light from the laser as eYFP-control mice did not exhibit any changes in rebound pressing ($t(4) = 0.0308$, $p = 0.488$). To address potential confounds related to light delivery, AAV5-EF1α-DIO-eYFP controls (n = 5) were tested on the 30s PI procedure using identical optogenetic conditions. Control mice did not exhibit any significant differences across trial types (Figure 6).

Lastly, we investigated how the length of optical inhibition modulates timing behavior at all three time points. For optical inhibition at trial onset (t = 0s), a repeated measures ANOVA found a significant main effect of stimulation length ($F(2, 8) = 9.845$, $p = 0.007$). Post tests found a significant difference between 15s of inhibition and 5s ($t(8) = 4.291$, $p = 0.0079$) as well as 10s ($t(8) = 3.125$, $p = 0.0424$: Figure 7A). Moreover, inhibition at t = 15s demonstrated a significant treatment effect ($F(2, 8) = 30.21$, $p < 0.001$) with longer durations of MD inhibition leading to increases in variance. A post-hoc test found 15s inhibition to produce significantly greater increases in variance than 5s or 10s of inhibition ($t(8) = 7.394$, $p < 0.001$; $t(8) = 5.773$, $p = 0.001$), respectively (Figure 7B). Moreover, this finding aligns with single trial data demonstrating increases in the length of the high-state correlate with the length of optical inhibition that occurs over the pressing phase. A two-way repeated measures ANOVA revealed a significant main effect of stim length on percent of rebound trials ($F(2, 8) = 5.199$, $p = 0.036$). Additionally, a Bonferroni corrected multiple comparison posttest found inhibition lengths of 15s ($t(8) = 5.526$, $p = 0.002$) and 10s ($t(8) = 4.435$, $p = 0.007$) result in a significantly greater percent of rebound trials than non-inhibition trials. Additionally, the 5s inhibition condition did not significantly increase rebound pressing ($t(8) = 1.56$, $p = 0.472$) despite the same length of a visual distractor having been previously shown to modify timing behavior in rats performing a 30s PI procedure (Buhusi and Meck, 2006).

Materials and Methods:

Viral Constructs

AAV5-EF1α-DIO-eNpHR3.0-eYFP and AAV5-EF1α-DIO-eYFP were obtained from the Duke Vector Core.

Animals

Data for pharmacological (n = 10) was collected from adult wild-type mice (C57BL/6). Optogenetic experiments used adult *Vglut2-IRES-Cre* (n = 11). In all behavioral experiments, mice were maintained on a 12:12 light cycle. During training of 30s peak interval procedure animals were food deprived, receiving 2.0-2.5 grams of rodent chow in addition to food pellets during testing. During food deprivation animal's weights were monitored daily to ensure they remained above 85% of baseline. All experimental procedures were approved by the Duke University Institutional Animal Care and Use Committee.

Surgery

Mice were anesthetized with 1.0 to 2.0% isoflurane mixed with 1.0 L/min of oxygen for surgical procedures and placed into a stereotactic frame (David Kopf Instruments, Tujunga, CA). Adult *Vglut2-IRES-Cre* mice were randomly assigned to Vglut2::eNpHR3.0 (n = 6) or Vglut2::eYFP groups (n = 5). Virus was bilaterally microinjected into the MD (0.3 μL each hemisphere, AP: −1.4 mm, ML: ± 1.48 mm, DV: −3.3 mm from skull surface, at 20° from vertical). All measurements are relative to bregma. Mice were bilaterally implanted with custom made fiber optics aimed directly above the MD (AP: −1.4 mm relative to bregma, ML: ± 1.48 mm, DV: −3.1 mm from skull surface, at 20° from vertical). Fibers were secured in place with dental acrylic adhered to skull screws. Mice were singly housed during recovery for at least two weeks before training began.

Peak Interval Training:

Lever-Press Training

Lever-Press training consisted of the extension a single lever, either to the right or left of a food port. A food pellet reward (Bio-Serv 20 mg Dustless Precision Pellet) was delivered for each lever press (FR-1). Every 5th press lead to an alternation of which lever was extended. Sessions ended after either successfully receiving 40 rewards or 30 min. Training was considered complete after an animal received 40 rewards prior to the 30 min time limit.

Fixed-Interval (FI) Training

FI training sessions began with the extension of a single lever to either the left or right of the food port, counterbalanced across mice, as well as the illumination of a house light. Individual trials were demarcated by the presence of an auditory cue (white noise; 68 dB). An animal was rewarded for the first lever press occurring after the cue had been on for 30 s. At this time a food reward was delivered, the cue was turned off, and the session entered a variable inter-trial interval ranging from 90 s to 180 s randomly selected from a uniform distribution of values in 5 s increments. If there was no press within 8-seconds of the 30 s criterion, the trial would end as stated above, but without a reward. There was no penalty for presses occurring prior to 30 s. The development of a "scalloped" profile for session averaged lever pressing indicated the acquisition of the to-be-learned interval and animals were transitioned to the final stage of training. Each session lasted 2 hrs.

Peak-Interval (PI) Training:

PI training sessions consisted of two trial types: The aforementioned FI trials, and unrewarded probe trials. During probe trials, the house light was turned on for a minimum of 3× the longer target duration (90 s) plus an additional random amount of time with a mean of 20 s and a Gaussian distribution. Each trial was randomly selected, with a 40% chance of being a probe trial. Each session lasted for 2 ½ hrs.

Local Muscimol Infusions

Mice received local bilateral infusions of either 0.9% saline or muscimol (0.01 mg/ml) solution. All infusions contained a total volume of 400nL (i.e. 200nL per hemisphere) infused at a rate of 0.05 mL/hr. Infusion cannulas were left in place for 10 min post infusion. After removal of cannulas, animals were again given 10 min prior to starting any training. The condition order was counterbalanced across animals. Control sessions consisted of insertion of injector cannula, but without infusing any solution. The injectors were left in place for 10 min and animals were given 10 min after removal before starting any training.

Optogenetic Stimulation

Optical stimulation began after an animal had progressed to the PI procedure and developed a distinctive peak in pressing activity centered around 30 s. Mice were connected to a 589-nm DPSS laser (Shanghai Laser) via fiber optic cables (Doric: core = 200μm; NA = 0.22) and placed inside the testing chamber (Rossi et al., 2012; Rossi et al., 2015). A rotating optical commutator (Doric) divided the beam (50:50) permitting bilateral stimulation. Stimulation (5-8 mW; constant; 15s, 10s, or 5s duration) was delivered at three timepoints: cue onset (t = 0), 15s after cue onset (t = 15), or 60s after cue onset (t = 60). The first two conditions occurred on both FI and probe trials, while the final condition only occurred on probe trials. The time of stimulation was held constant within a session but varied across sessions.

Histology

After testing was completed, mice were deeply anesthetized with isoflurane and perfused with 0.1M PBS followed by 4% paraformaldehyde. Brains were post fixed in 4% paraformaldehyde for 24hrs followed by 30% sucrose. After sinking in the sucrose solution, brains were sliced coronally at 60 μm using a Leica CM1850 cryostat. For cannula localization, sections were mounted and immediately coverslipped with Fluoromount G with DAPI medium (Electron Microscopy Sciences; catalog #17984-24). Placement was validated using an Axio Imager.V16 upright microscope (Zeiss). For visualization of viral expression and fiber placement, fluorescent images were taken with a Z10 inverted microscope (Zeiss). To confirm proper fiber placement, sections compared to images from a mouse brain atlas (Paxinos & Franklin, 2019).

Data Collection and Statistical Analysis

Experimental procedures were controlled by a MED Associates interface utilizing MED-PC software system. Lever presses were recorded in real time with 10 millisecond resolution. Session averaged data was analyzed using in-house Python scripts. All statistical analysis was performed in Prism 8.

Session Data Analysis

Lever pressing data for each trial was placed into 2s bins and collapsed across all trials. The cumulative pressing data was smoothed using a Savitzky-Golay filter and then fit using a gaussian curve with the addition of a linear ramp accommodating the right-tail skew, resulting from the temporal asymmetry of expected reward time relative to length of probe trials. Fits were used to obtain peak times (accuracy) and peak spread (precision) as previously described (Cheng and Meck, 2007). For optogenetic experiments fits where calculated by combining data from two sessions in order to provide a sufficient number of trials for single trial analysis, because only about half the trials of each session were stimulation trials.

Single Trial Analysis

Lever pressing data for an individual trial was first placed into 1s bins. As the probe trials were of variable length with a minimum duration of 90s only the first 90 bins were included. The press-rate data was padded on both sides and smoothed using a median filter, followed by a Savitzky-Golay filter. The smoothed data was log normalized and then change points were detected using python ruptures library with a Pelt search method and “L2” cost function. To account for differences in press rate between animals, the penalty and median filter length values were allowed to vary.

Discussion:

Despite evidence implicating elapsed time as constituting an inherent neuro-computational process tied into MD associated networks, its role in temporally guided behavior is unclear (Mitchell et al., 2014). Utilizing pharmacological and optogenetic manipulations, we provide evidence for the involvement of the MD in interval timing on a free operant task. By inhibiting MD activity during distinct phases of a temporal reproduction task, we show systematic delays in the transition between behaviors. Investigation of both total lever-pressing and pressing sequences show the effects are not confounded by changes in motor output, but likely through internal timing mechanisms.

Reversible pharmacological inhibition of the MD disrupts the accuracy and precision of lever pressing in mice performing a multi-second temporal production task (Figure 1-2). To further dissect MD involvement in various stages of timing behavior, we employed optogenetic techniques at various time points throughout individual trials. Inhibition of the MD was found to produce preservation of current behavior during a trial resulting in delays in the onset of pressing for inhibition at t = 0 (Figure 3) and offset of pressing at t = 15 (Figure 4). Moreover, these effects were found to be proportionate to the length of optical inhibition. These findings elucidate how animals time individual components of the task. During a probe trial, one stratagem a mouse may use is to time the 30s criterion duration while having a sense of it being almost 30s or past 30s. Alternatively, the mouse may time how long to wait to press and then time how long to press. Here we show that the length of inhibition during the 'high-state' strongly correlates with the increase in length of the pressing bout. This provides evidence in support for the second strategy. Therefore, dissociable behavioral effects related to timing of inhibition relative to ongoing behavior suggests the MD assists in maintaining veridical temporal representations during each stage of a temporal reproduction task.

As timing signatures have been found across many cortical regions, a promising theoretical role of the thalamus is through modulating the functional connectivity within and across cortical areas, with the MD dedicated to the PFC (Jones, 2012). In fact, connectivity between these brain regions has been likened to a coincidence detection network suggested to regulate neural oscillations, synchrony and resonance (Jones E. G., 2002). Therefore, down regulation or desynchronization of any one region (i.e. PL) is insufficient to disrupt interval timing behavior as long as the MD is able to coordinate the timing information amongst a sufficient number of other areas.

Substantial evidence supports the role of higher-order thalamic nuclei, such as the MD, in synchronizing neural activity within the cortex (Theyel et al., 2010; Saalmann, 2014). The MD supports internal monitoring of movement sequences in the PFC through corollary discharge. In non-human primates performing a sequential saccade task, muscimol inactivation of the MD prevented effective compensation in the direction of a second saccade relative to the first (Sommer and Wurtz, 2002). It has been argued that working memory and interval timing share underlying neural mechanisms (Matell et al., 2005).

Similarly, many theoretical models of timing rely on the synchronization, coordination, or integration of temporal information from distributed sources (Hass and Durstewitz, 2016; Petter et al., 2016). For example, the striatal beat frequency (SBF) model proposes that neural oscillators in the cortex are synchronized at the onset of a to-be-timed interval and time can be tracked through the changes in their phase relationship over time (Matell & Meck, 2004). While the SBF has suggested dopamine signaling as a potential mechanism for synchronization, the MD is particularly well situated to participate in this role. Though more robust in humans and non-human primates, the rodent MD receives convergent inputs from subcortical limbic structures that overlap with dopaminergic innervation and recordings show dopamine can modulate responsivity of MD cells (Lavin and Grace, 1998). Moreover, pharmacological inhibition of the MD resulted in decreased dopamine transmission in the PFC (Churchill et al., 1996) a condition that has been associated with decreases in 'clock speed' and increases in temporal uncertainty (Cheng et al., 2016), and in line with the findings presented here. Therefore, the MD appears to be a critical component of the timing circuit.

Previous work showed that activating GABAergic outputs from the substantia nigra pars reticulata to the deep layer of the superior colliculus (SC) not only leads to a pause in ongoing behavior, but delays subsequent anticipatory timing behavior (Toda et al., 2017). Also receiving direct projections from the SNr, the MD may play a vital role in integrating timing signals in the PFC (Haber et al., 1985; Groenewegen, 1988; Miyamoto and Jinnai, 1994).

In addition to facilitating the transfer of timing-related signals across brain regions, the MD may support timing through stabilizing activity within particular subregions. Activity in the MD has been shown to amplify local PFC connectivity, allowing for the emergence of specific neural sequences. Increasing the excitatory to inhibitory (E/I) ratio in the PFC can mitigate this amplification leading to deceased performance on two-alternative forced choice task.

Pathological disruptions in thalamocortical interactions exhibit these elevated E/I ratios and result in attentional deficits as well as impairments in interval timing (Ward et al., 2012). Previous timing research has shown challenges to timing networks requiring attentional and/or memory resources can lead to delays in peak time and, importantly, the shift is proportional to the salience of the perturbation (Buhusi and Meck, 2009). This is indeed what we observed in the current study, with the magnitude of deviation from non-stimulation trials being proportional to the length of MD inhibition.

In summary, using pharmacological and optogenetic inhibition of MD activity, we found for the first time a key role of this thalamic nucleus in interval timing. As the MD is a crucial node connecting basal ganglia outputs and the prefrontal cortex, our result complement previous work on the contributions of these structures in timing.

Acknowledgments

We would like to dedicate this paper to the memory of our co-author Warren H. Meck, a pioneer in the study of interval timing, who passed away unexpectedly during the preparation of the manuscript. This research was supported by DA040701, MH112883, and NS094754 to HHY.

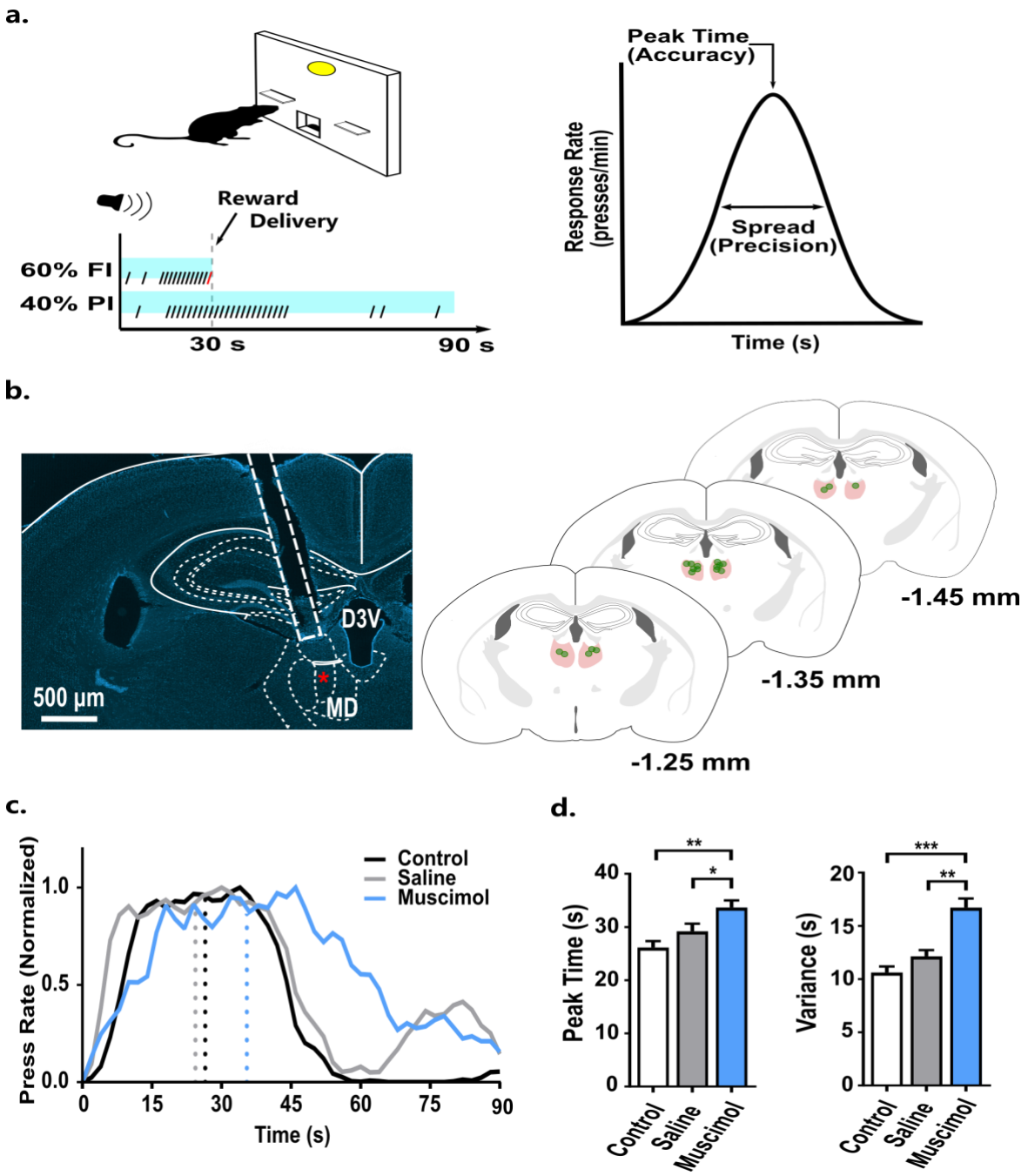

Figure 1: Pharmacological inhibition of MD disrupts interval timing behavior. (a) Schematic of behavioral task and idealized behavioral output. (b) Location of cannula placement. Infusion canula (red asterisk) located 0.5mm below guide canula (white box). (c) Representative performance of a mouse under control (black), saline (grey), and muscimol (blue) conditions. Dotted lines indicate peak times defined by Gaussian + Ramp fit. (d) Muscimol has effects on timing performance, from left to right: peak time, variance across, and elevation ratios. *$p < 0.05$, ** $p < 0.01$, *** $p < 0.001$.

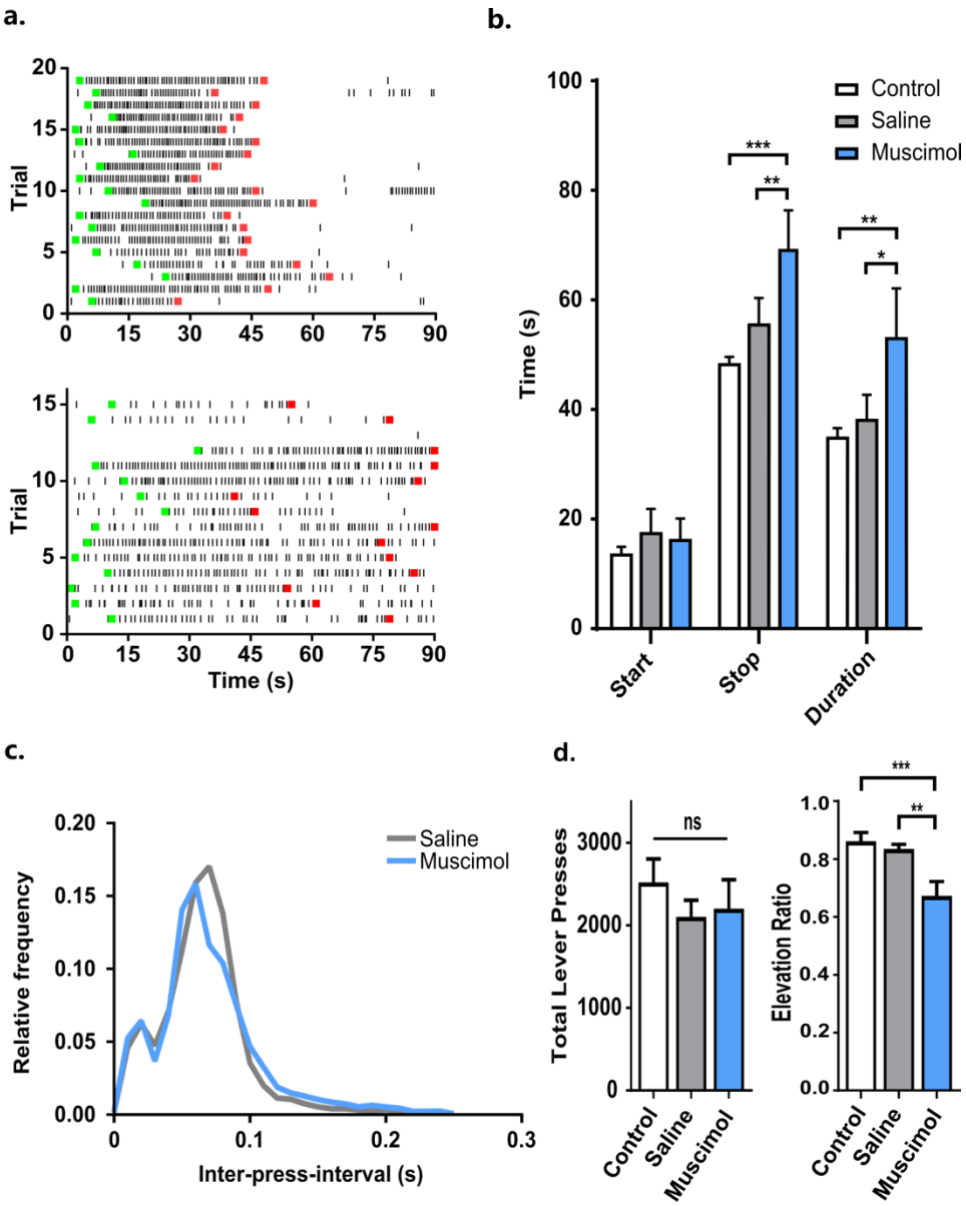

Figure 2: Single trial analysis demonstrates differences in pressing profiles. (a) Representative raster plot of individual trials during control (top) and muscimol (bottom) conditions. Each black dash represents a single lever press. Green and red squares indicate the start and stop times, respectively (see Methods). (b) Average start time, stop time, and duration of pressing bout for mice across conditions (c) Histogram of inter-press-intervals (IPIs) across conditions. (d) total lever presses (left) and elevation ratio (right) during a session. * $p < 0.05$, ** $p < 0.01$, *** $p < 0.001$

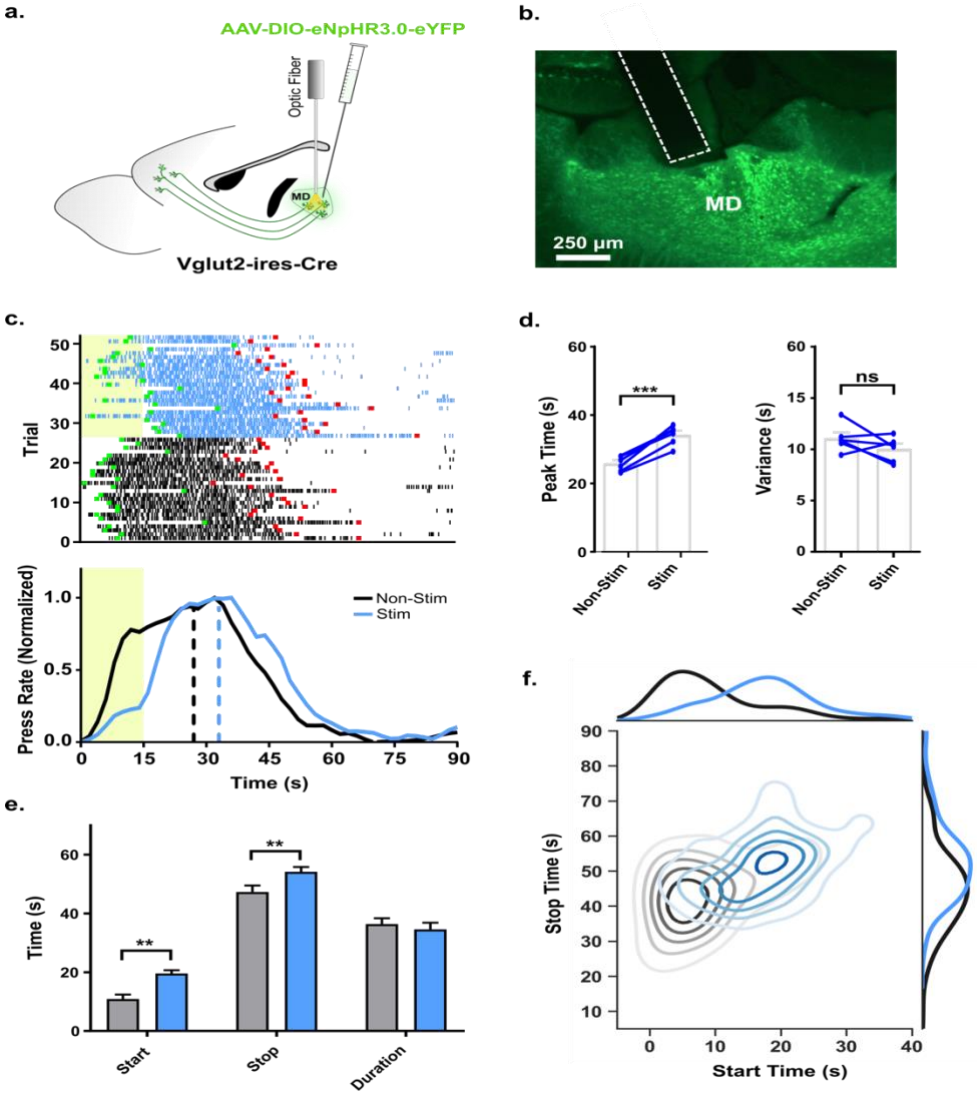

Figure 3: Optical inhibition of MD at cue onset delays initiation of lever pressing. (a) Schematic of viral infection and fiber optic implantation. (b) Histology demonstrating viral expression and fiber placement in MD (c) Example of single trial (top) and averaged (bottom) pressing data over two sessions with 15s stimulation at onset of auditory cue (yellow rectangle). Each tick represents a single lever press. Green and red squares indicate the start and stop times, respectively. Dashed lines indicate peak time of gaussian + ramp fit (d) Stimulation delays peak time (left) but not variance (right) of peak fits. Group average (grey) and individual (blue) data shown. (e) Stimulation significantly affects average start time and stop time, but not press bout duration (f) Distributions of start and stop times for all trials. ** $p < 0.01$, *** $p < 0.001$

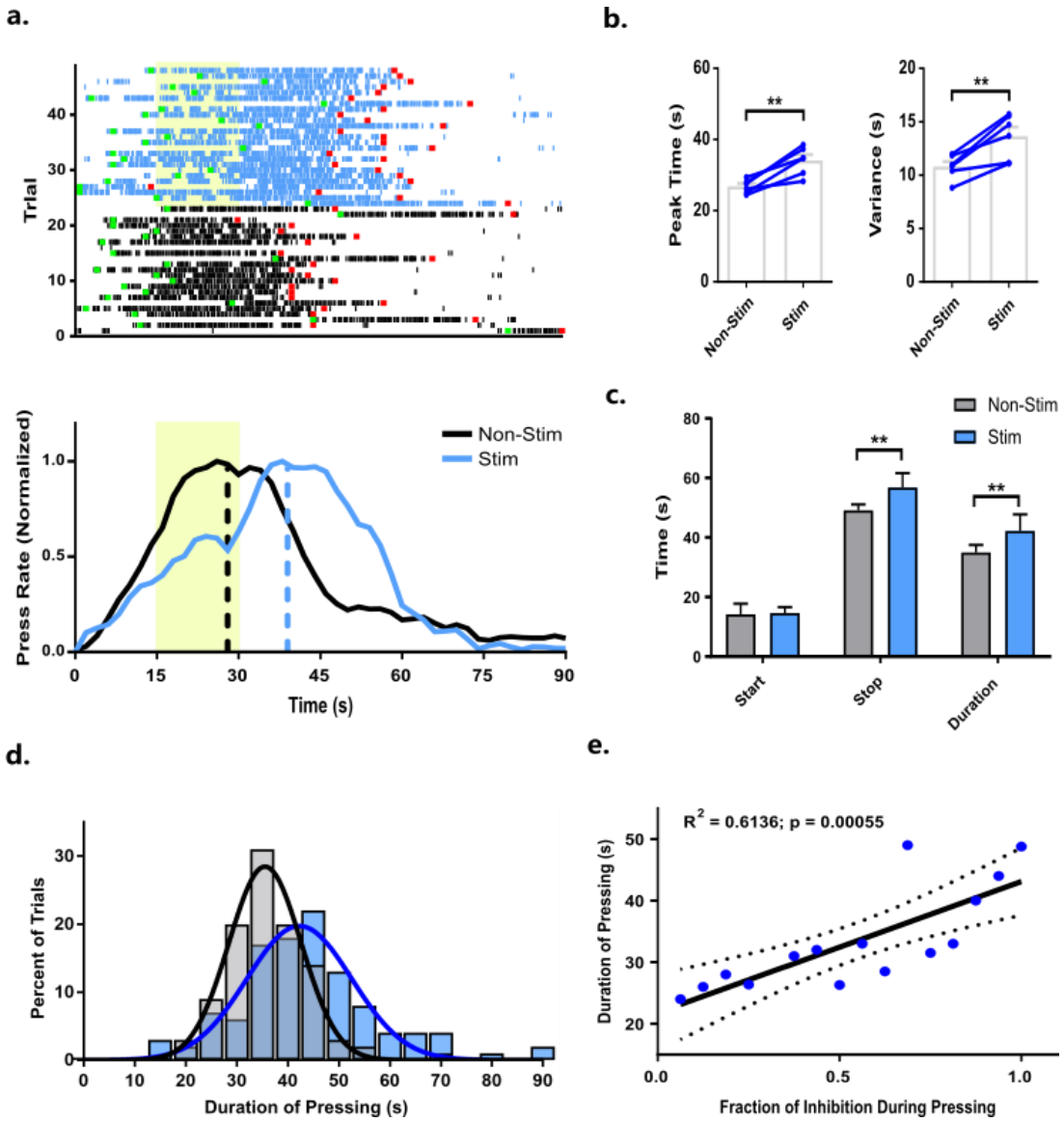

Figure 4: Optical inhibition of MD during pressing increases length of pressing bout (a) Example of single trial (top) and averaged (bottom) pressing data over two sessions with 15s stimulation at onset of auditory cue (yellow rectangle). Each tick represents a single lever press. Green and red squares indicate the start and stop times, respectively. Dashed lines indicate peak time of gaussian + ramp fit (b) Stimulation delays peak time (left) and variance (right) of peak fits. Group average (grey) and individual (blue) data shown. (c) Stimulation significantly affects average start time and stop time, but not press bout duration (d) histogram of press durations for stim and non-stim trials. (e) Linear regression of press duration relative to percent of the total stim time received *$p < 0.05$, ** $p < 0.01$

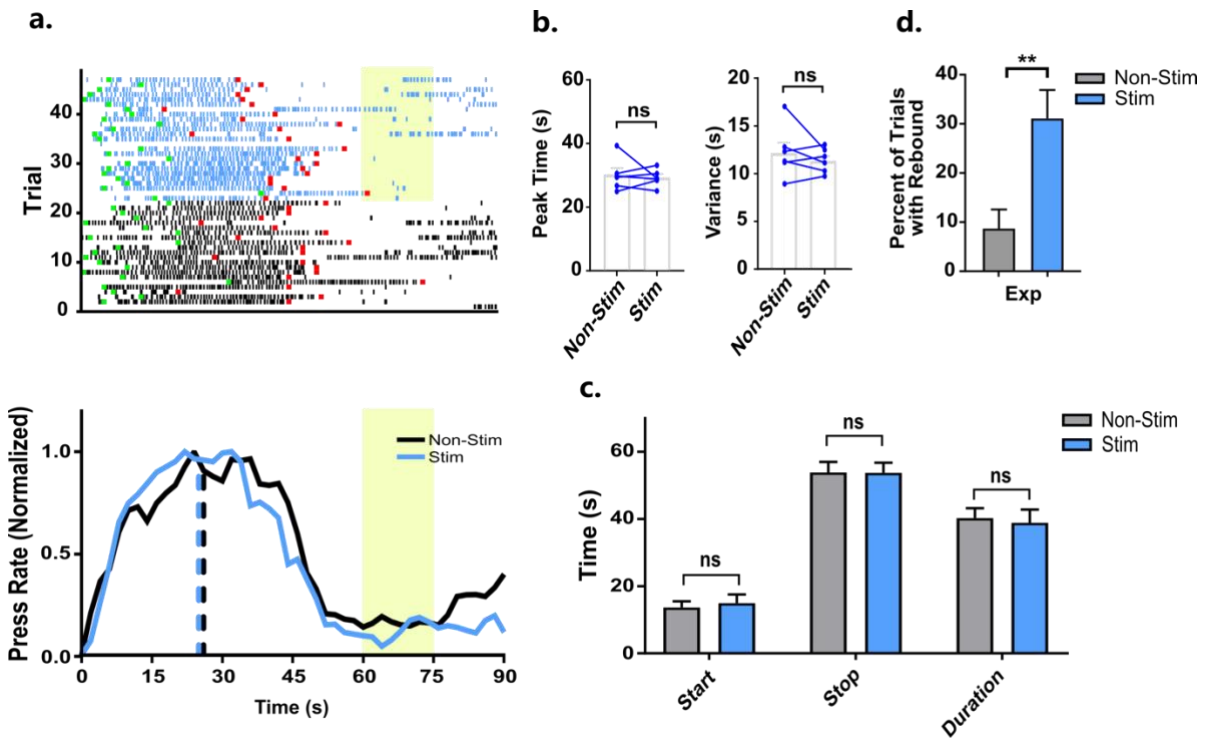

Figure 5: Optical inhibition following pressing increases probability of reengagement (a) Example of single trial (top) and averaged (bottom) pressing data over two sessions with 15s stimulation at t = 60s of auditory cue (yellow rectangle). Each tick represents a single lever press. Green and red squares indicate the start and stop times, respectively. Dashed lines indicate peak time of gaussian + ramp fit (b) Stimulation has no effect on peak time (left) or variance (right) of peak fits. Group average (grey) and individual (blue) data shown. (c) Stimulation has no significant affect start time and stop time, or press bout duration. (d) Percent of trials with reengagement (rebound). ** $p < 0.01$

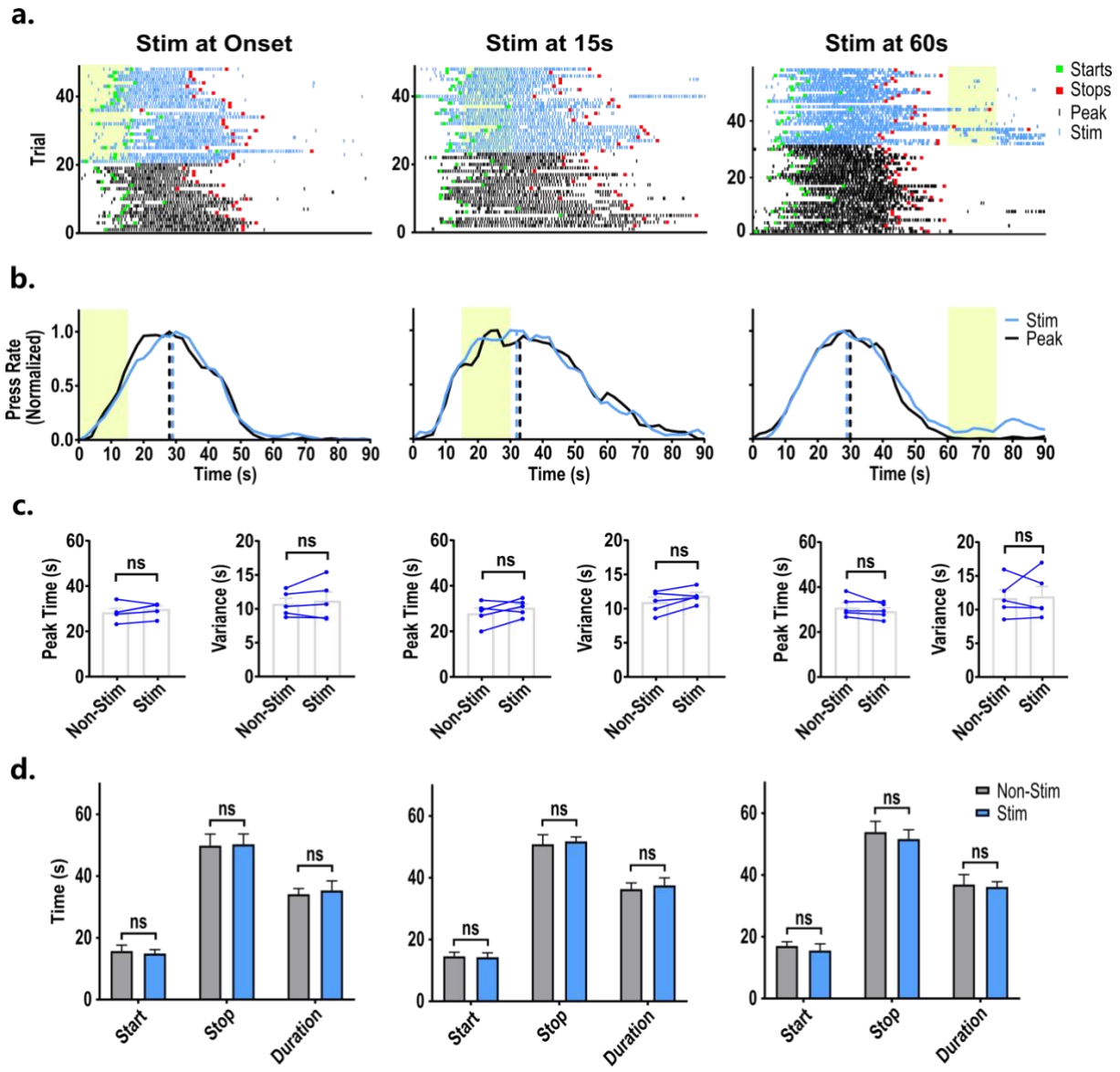

Figure 6: No changes in behavior for eYFP controls (a) Raster plots for eYFP control animals for stim (blue) and non-stim (black) trials at timepoints, from left to right, t = 0s, t = 15s, and t = 60s (yellow). (b) Session averaged data for eYFP control animals for stim (blue) and non-stim (black) trials at timepoints, from left to right, t = 0s, t = 15s, and t = 60s (yellow). Peak times for stim (blue dash) and non-stim (black dash) defined by Gaussian + Ramp fits. (c) Stimulation does not modify peak time (left) or variance (right) of peak fits. Group average (grey) and individual (blue) data shown. (d) Stimulation has no significant affect average start time and stop time, or press bout duration.

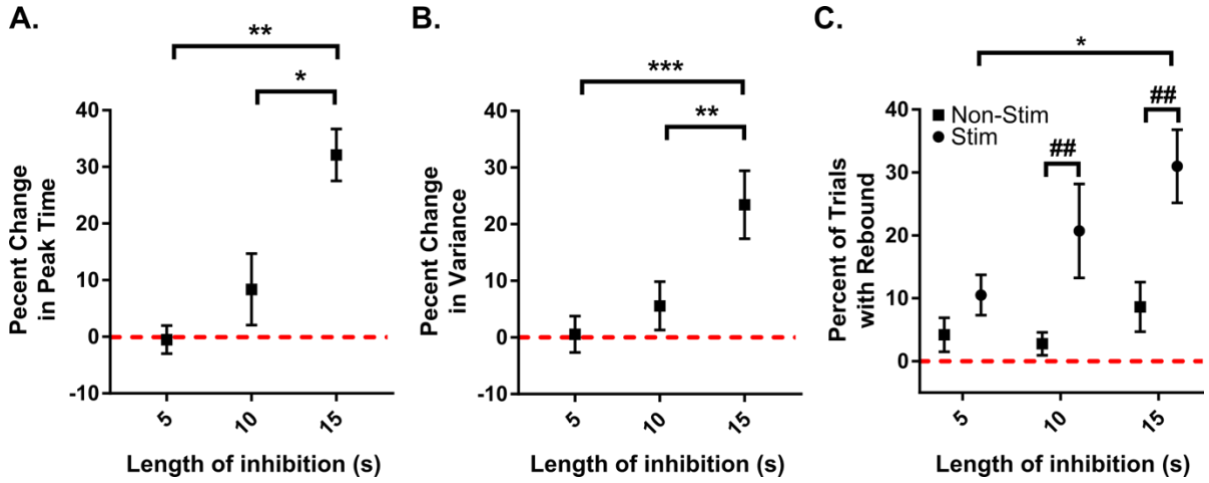

Figure 7: Effects of optical inhibition scale with length of inhibition. (a) Percent increase in session peak time relative to length of optical inhibition at t = 0s. (b) Percent increase in session variance relative to length of optical inhibition at t = 15s. (c) Percent of trial with rebound pressing relative to length of optical inhibition at t = 60s.

References

Bakhurin KI, Goudar V, Shobe JL, Claar LD, Buonomano DV, Masmanidis SC (2017) Differential Encoding of Time by Prefrontal and Striatal Network Dynamics. The Journal of neuroscience : the official journal of the Society for Neuroscience 37:854-870.

Bolkan SS, Stujenske JM, Parnaudeau S, Spellman TJ, Rauffenbart C, Abbas AI, Harris AZ, Gordon JA, Kellendonk C (2017) Thalamic projections sustain prefrontal activity during working memory maintenance. Nature neuroscience 20:987.

Buhusi CV, Meck WH (2005) What makes us tick? Functional and neural mechanisms of interval timing. Nature reviews Neuroscience.

Buhusi CV, Meck WH (2009) Relativity theory and time perception: single or multiple clocks? PloS one 4.

Buhusi CV, Reyes MB, Gathers C-A, Oprisan SA, Buhusi M (2018) Inactivation of the medial-prefrontal cortex impairs interval timing precision, but not timing accuracy or scalar timing in a peak-interval procedure in rats. Frontiers in Integrative Neuroscience 12:20.

Buhusi CV, Aziz D, Winslow D, Carter RE, Swearingen JE, Buhusi MC (2009) Interval timing accuracy and scalar timing in C57BL/6 mice. Behav Neurosci 123:1102-1113.

Cheng R-K, Meck WH (2007) Prenatal choline supplementation increases sensitivity to time by reducing non-scalar sources of variance in adult temporal processing. Brain research 1186:242-254.

Cheng R-K, Tipples J, Narayanan NS, Meck WH (2016) Clock speed as a window into dopaminergic control of emotion and time perception. Timing & Time Perception 4:99-122.

Church RM, Meck WH, Gibbon J (1994) Application of scalar timing theory to individual trials. Journal of Experimental Psychology: Animal Behavior Processes 20:135.

Churchill L, Zahm D, Duffy P, Kalivas P (1996) The mediodorsal nucleus of the thalamus in rats—II. Behavioral and neurochemical effects of GABA agonists. Neuroscience 70:103-112.

Corbit LH, Muir JL, Balleine BW (2003) Lesions of mediodorsal thalamus and anterior thalamic nuclei produce dissociable effects on instrumental conditioning in rats. The European journal of neuroscience 18:1286-1294.

Delevich K, Tucciarone J, Huang ZJ, Li B (2015) The mediodorsal thalamus drives feedforward inhibition in the anterior cingulate cortex via parvalbumin interneurons. Journal of Neuroscience 35:5743-5753.

Ferguson BR, Gao W-J (2018) Thalamic control of cognition and social behavior via regulation of gamma-aminobutyric acidergic signaling and excitation/inhibition balance in the medial prefrontal cortex. Biological psychiatry 83:657-669.

Finnerty GT, Shadlen MN, Jazayeri M, Nobre AC, Buonomano DV (2015) Time in cortical circuits. Journal of Neuroscience 35:13912-13916.

Gouvea TS, Monteiro T, Motiwala A, Soares S, Machens C, Paton JJ (2015) Striatal dynamics explain duration judgments. eLife 4.

Groenewegen H (1988) Organization of the afferent connections of the mediodorsal thalamic nucleus in the rat, related to the mediodorsal-prefrontal topography. Neuroscience 24:379-431.

Haber SN, Groenewegen HJ, Grove EA, Nauta WJ (1985) Efferent connections of the ventral pallidum: evidence of a dual striato pallidofugal pathway. The Journal of comparative neurology 235:322-335.
Hass J, Durstewitz D (2016) Time at the center, or time at the side? Assessing current models of time perception. Current Opinion in Behavioral Sciences 8:238-244.
Heidbreder CA, Groenewegen HJ (2003) The medial prefrontal cortex in the rat: evidence for a dorso-ventral distinction based upon functional and anatomical characteristics. Neuroscience & Biobehavioral Reviews 27:555-579.
Jones CR, Rosenkranz K, Rothwell JC, Jahanshahi M (2004) The right dorsolateral prefrontal cortex is essential in time reproduction: an investigation with repetitive transcranial magnetic stimulation. Experimental Brain Research 158:366-372.
Jones EG (2012) The thalamus: Springer Science & Business Media.
Kim J, Ghim J-W, Lee JH, Jung MW (2013) Neural correlates of interval timing in rodent prefrontal cortex. Journal of Neuroscience 33:13834-13847.
Kim Y-C, Narayanan NS (2019) Prefrontal D1 dopamine-receptor neurons and delta resonance in interval timing. Cerebral Cortex 29:2051-2060.
Lavin A, Grace A (1998) Dopamine modulates the responsivity of mediodorsal thalamic cells recorded in vitro. Journal of Neuroscience 18:10566-10578.
Lewis PA, Miall RC (2003) Distinct systems for automatic and cognitively controlled time measurement: evidence from neuroimaging. Current opinion in neurobiology 13:250-255.
Matell MS, Meck WH, Lustig C (2005) Not “just” a coincidence: Frontal-striatal interactions in working memory and interval timing. Memory 13:441-448.
Meck WH (2006) Neuroanatomical localization of an internal clock: a functional link between mesolimbic, nigrostriatal, and mesocortical dopaminergic systems. Brain Res 1109:93-107.
Mitchell AS, Sherman SM, Sommer MA, Mair RG, Vertes RP, Chudasama Y (2014) Advances in understanding mechanisms of thalamic relays in cognition and behavior. Journal of Neuroscience 34:15340-15346.
Miyamoto Y, Jinnai K (1994) The inhibitory input from the substantia nigra to the mediodorsal nucleus neurons projecting to the prefrontal cortex in the cat. Brain research 649:313-318.
Ostlund SB, Balleine BW (2008) Differential involvement of the basolateral amygdala and mediodorsal thalamus in instrumental action selection. The Journal of neuroscience : the official journal of the Society for Neuroscience 28:4398-4405.
Parnaudeau S, Taylor K, Bolkan SS, Ward RD, Balsam PD, Kellendonk C (2015) Mediodorsal thalamus hypofunction impairs flexible goal-directed behavior. Biological psychiatry 77:445-453.
Parnaudeau S, O’Neill P-K, Bolkan SS, Ward RD, Abbas AI, Roth BL, Balsam PD, Gordon JA, Kellendonk C (2013) Inhibition of mediodorsal thalamus disrupts thalamofrontal connectivity and cognition. Neuron 77:1151-1162.
Petter EA, Lusk NA, Hesslow G, Meck WH (2016) Interactive roles of the cerebellum and striatum in sub-second and supra-second timing: Support for an initiation, continuation, adjustment, and termination (ICAT) model of temporal processing. Neuroscience & Biobehavioral Reviews 71:739-755.
Rossi MA, Calakos N, Yin HH (2015) Spotlight on movement disorders: what optogenetics has to offer. Movement Disorders 30:624-631.

Rossi MA, Hayrapetyan VY, Maimon B, Mak K, Je HS, Yin HH (2012) Prefrontal cortical mechanisms underlying delayed alternation in mice. Journal of neurophysiology 108:1211-1222.
Saalmann YB (2014) Intralaminar and medial thalamic influence on cortical synchrony, information transmission and cognition. Frontiers in systems neuroscience 8:83.
Sommer MA, Wurtz RH (2002) A pathway in primate brain for internal monitoring of movements. Science 296:1480-1482.
Teki S, Grube M, Griffiths TD (2012) A unified model of time perception accounts for duration-based and beat-based timing mechanisms. Frontiers in integrative neuroscience 5:90.
Theyel BB, Llano DA, Sherman SM (2010) The corticothalamocortical circuit drives higher-order cortex in the mouse. Nature neuroscience 13:84-88.
Tiganj Z, Jung MW, Kim J, Howard MW (2017) Sequential firing codes for time in rodent medial prefrontal cortex. Cerebral Cortex 27:5663-5671.
Toda K, Lusk NA, Watson GDR, Kim N, Lu D, Li HE, Meck WH, Yin HH (2017) Nigrotectal Stimulation Stops Interval Timing in Mice. Current biology : CB 27:3763-3770 e3763.
Wang J, Narain D, Hosseini EA, Jazayeri M (2018) Flexible timing by temporal scaling of cortical responses. Nature neuroscience 21:102-110.
Ward RD, Kellendonk C, Kandel ER, Balsam PD (2012) Timing as a window on cognition in schizophrenia. Neuropharmacology 62:1175-1181.
Yin HH (2014) Action, time and the basal ganglia. Philosophical Transactions of the Royal Society B: Biological Sciences 369.
Yu C, Gupta J, Yin HH (2010) The role of mediodorsal thalamus in temporal differentiation of reward-guided actions. Front Integr Neurosci 4.
Yu C, Fan D, Lopez A, Yin HH (2012) Dynamic changes in single unit activity and gamma oscillations in a thalamocortical circuit during rapid instrumental learning. PLoS One 7:e50578.
Zhang F, Wang L-P, Brauner M, Liewald JF, Kay K, Watzke N, Wood PG, Bamberg E, Nagel G, Gottschalk A (2007) Multimodal fast optical interrogation of neural circuitry. Nature 446:633-639.